# CORRESPONDENCE

## Comments on "Combination Mode Dynamics of the Anomalous Northwest Pacific Anticyclone"*

TIM LI, BIN WANG, AND LU WANG

*Key Laboratory of Meteorological Disaster of Ministry of Education, Joint International Research Laboratory of Climate and Environmental Change, and Collaborative Innovation Center on Forecast and Evaluation of Meteorological Disasters, Nanjing University of Information Science and Technology, Nanjing, China, and International Pacific Research Center and Department of Atmospheric Sciences, School of Ocean and Earth Science and Technology, University of Hawai'i at Mānoa, Honolulu, Hawaii*

(Manuscript received 30 May 2015, in final form 29 February 2016)

ABSTRACT

In a recent paper, Stuecker et al. applied a "combination mode" (C-mode) theory to explain the formation of the anomalous western North Pacific anticyclone (WNPAC) during El Niño events. The C-mode, arising from interaction between the annual cycle and ENSO, is an Indo-Pacific basin mode with two "near annual" time scales (roughly 10 and 15 months, respectively). This comment discusses to what extent the C-mode can explain the WNPAC dynamics. The major findings are the following: 1) spectral analysis of the Indo-Pacific circulation anomaly fields indicates that the 10-month mode is not observed and the 15-month mode is only seen in the western North Pacific (WNP), where its spectral peak is statistically insignificant; 2) the 15-month mode (with a period of 13–19 months) accounts for only a small portion (13%) of the observed sea level pressure anomaly in the WNP; and 3) the C-mode evolution does not capture the observed timing of the WNPAC onset in the northern fall of El Niño developing year. In addition it is shown, based on observational analyses and numerical experiments, that local atmosphere–ocean interaction plays an important role in formation of the anomalous anticyclonic center over the Philippine Sea.

### 1. Introduction

Investigation of anomalous western North Pacific anticyclone (WNPAC) variation is of utmost importance for understanding the variation and prediction of the East Asian monsoon rainfall and tropical storm activities in the WNP (Wang et al. 2013). Extensive studies have been focused on the origin of the anomalous WNPAC associated with El Niño, and two mechanisms have been proposed to be critical in its development and maintenance. The first is the interaction between the WNPAC and underlying warm pool ocean through convectively coupled atmospheric Rossby waves interacting with ocean mixed layer in the presence of annual cycle of the mean flows (Wang et al. 2000, 2003; Lau et al. 2004; Lau and Wang 2006; Wu et al. 2010a; Chowdary et al. 2013; Kosaka et al. 2013; Xiang et al. 2013). The second highlights the importance of the delayed tropical Indian Ocean (IO) warming, which may force atmospheric Kelvin waves and result in equatorial easterly and associated anticyclonic shear vorticity in the WNP (Xie et al. 2009; Wu et al. 2009, 2010b; Chowdary et al. 2010, 2011).

A recent study by Stuecker et al. (2015, hereafter S15) proposed an alternative explanation of the WNPAC dynamics using a "combination mode" (C-mode) theory. The C-mode is, in essence, an amplitude modulation of the annual cycle by El Niño–Southern Oscillation (ENSO) (or vice versa) and thus it is an Indo-Pacific basin mode. The C-mode exhibits characteristic time scales (near-annual combination tones) of 10 and 15 months (Stuecker et al. 2013), which correspond respectively to frequencies of 1.2 and 0.8 $yr^{-1}$. The C-mode was claimed

* School of Ocean and Earth Science and Technology Publication Number 9606, International Pacific Research Center Publication Number 1182, and Earth System Modeling Center Contribution Number 98.

*Corresponding author address*: Tim Li, IPRC and Department of Atmospheric Sciences, University of Hawai'i at Mānoa, 2525 Correa Rd., Honolulu, HI 96822.
E-mail: timli@hawaii.edu

DOI: 10.1175/JCLI-D-15-0385.1

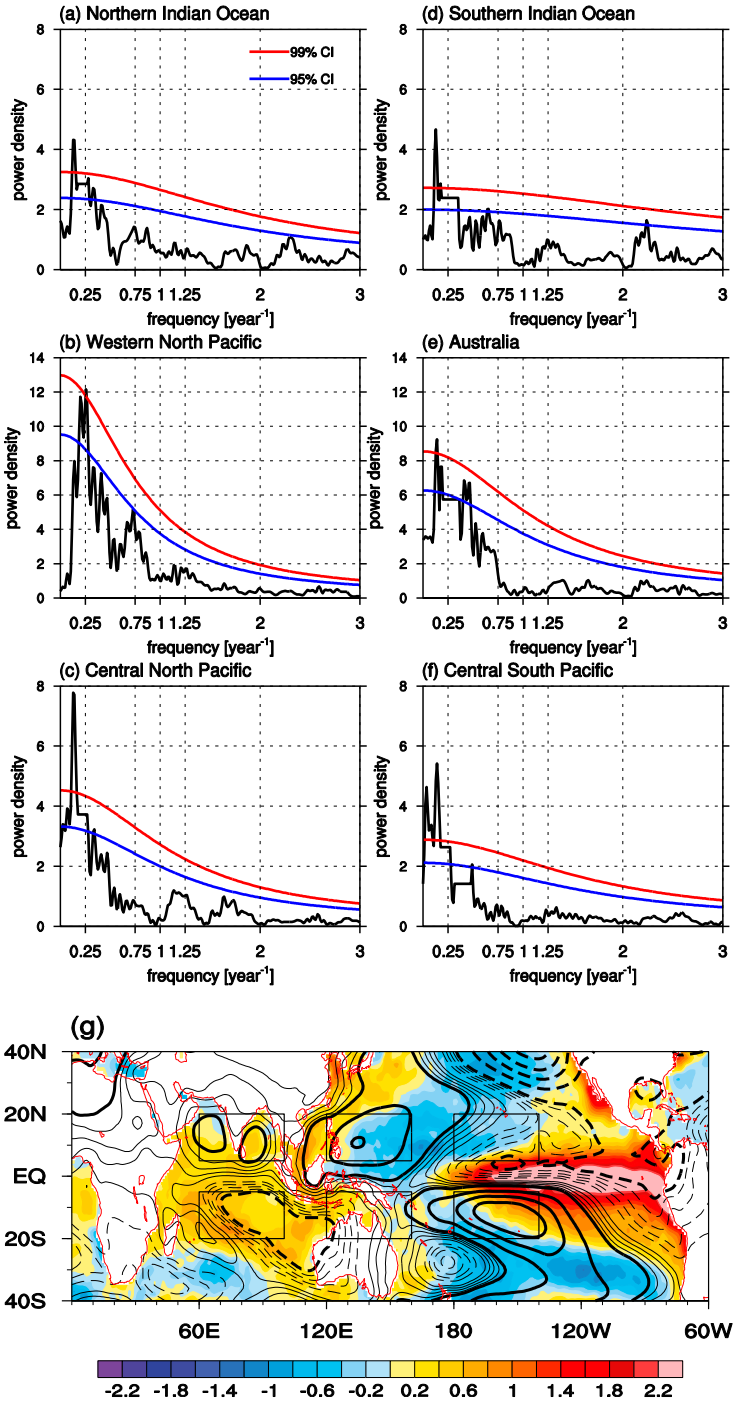


FIG. 1. Multitaper method (MTM) power spectra for sea level pressure (SLP) anomalies averaged over (a) the northern Indian Ocean (5°–20°N, 60°–100°E), (b) the western North Pacific (5°–20°N, 120°–160°E), (c) the central North Pacific (5°–20°N, 180°–140°W), (d) the southern Indian Ocean (20°–5°S, 60°–100°E), (e) Australia (20°–5°S, 120°–160°E), and (f) the central South Pacific (20°–5°S, 180°–140°W). Black lines indicate the power density and colored lines indicate the confidence interval (CI; red = 99% and blue = 95%) based on a red noise null hypothesis. (g) The regions for spectral analysis are outlined with black rectangles. Also shown are the observed composite pattern of SST anomalies (shading, °C) and 1000-hPa streamfunction anomalies (thin contour interval: $0.2 \times 10^6$ from $-0.8 \times 10^6$ to $0.8 \times 10^6$ m$^2$ s$^{-1}$ with zero line omitted and thick contour interval: $10^6$ m$^2$ s$^{-1}$) for El Niño peak phase (DJF) during 1980–2001.

to be "the main contributor to the time evolution of the antisymmetric anticyclonic and cyclonic circulation anomalies in the Indo-Pacific during both El Niño and La Niña events" (S15, p. 1095). S15 argued against the role of the delayed IO warming on WNPAC by stating that the observed WNPAC is highly meridionally asymmetric while the Kelvin wave response is symmetric about the equator. In addition, S15 concluded, without a quantitative measure, that the role of atmosphere–ocean interaction in the tropical IO and northwestern Pacific is of secondary importance in the development and maintenance of the WNPAC.

In S15, the theoretical C-mode was primarily compared with modeling experiments (e.g., their Figs. 3–11). In this paper we test the C-mode against observations. In the following sections we will examine, respectively, 1) whether the circulation anomalies in the WNPAC and tropical Indo-Pacific have statistically significant near-annual combination tones (section 2), 2) to what extent the near-annual variation can explain observed circulation variability in the WNP (section 3), 3) whether the C-mode captures the timing of the WNPAC onset during El Niño events (section 4), and 4) what role the local atmosphere–ocean interaction plays in WNPAC development (section 5). Through direct comparison with observations, we demonstrate that the theoretical C-mode proposed by S15 has difficulties in explaining the observed frequency, amplitude, and onset characteristics of the WNPAC.

## 2. Can C-mode frequencies be observed in the tropical Indo-Pacific circulation anomalies?

S15 claimed that "the associated near-annual time scale of the C-mode has been overlooked in the previous studies of Indo-Pacific climate" (p. 1095). Many previous studies of the Indo-Pacific climate have detected and well documented two modes of variability, the ENSO-related mode (e.g., Webster et al. 1998) and the tropospheric biennial oscillation (TBO; Nicholls 1978; Meehl 1987, 1994, 1997; Chang and Li 2000; Li et al. 2001, 2006). We are curious about how significant the C-mode frequencies are in observations.

To examine whether the near-annual frequencies predicted by the C-mode, namely, the $1.2\,\mathrm{yr}^{-1}$ (corresponding to a 10-month period) and $0.8\,\mathrm{yr}^{-1}$ (corresponding to a 15-month period), occur or not in the tropical Indo-Pacific regions, we examine the power spectrums of sea level pressure (SLP) anomalies in six selected regions that cover nearly the entire tropical Indo-Pacific (Fig. 1). To facilitate direct comparison with S15, the same ERA-40 reanalysis dataset (Uppala et al. 2005) for the same analysis period (1980–2001) and the same multitaper spectral analysis method (Ghil et al. 2002) were used.

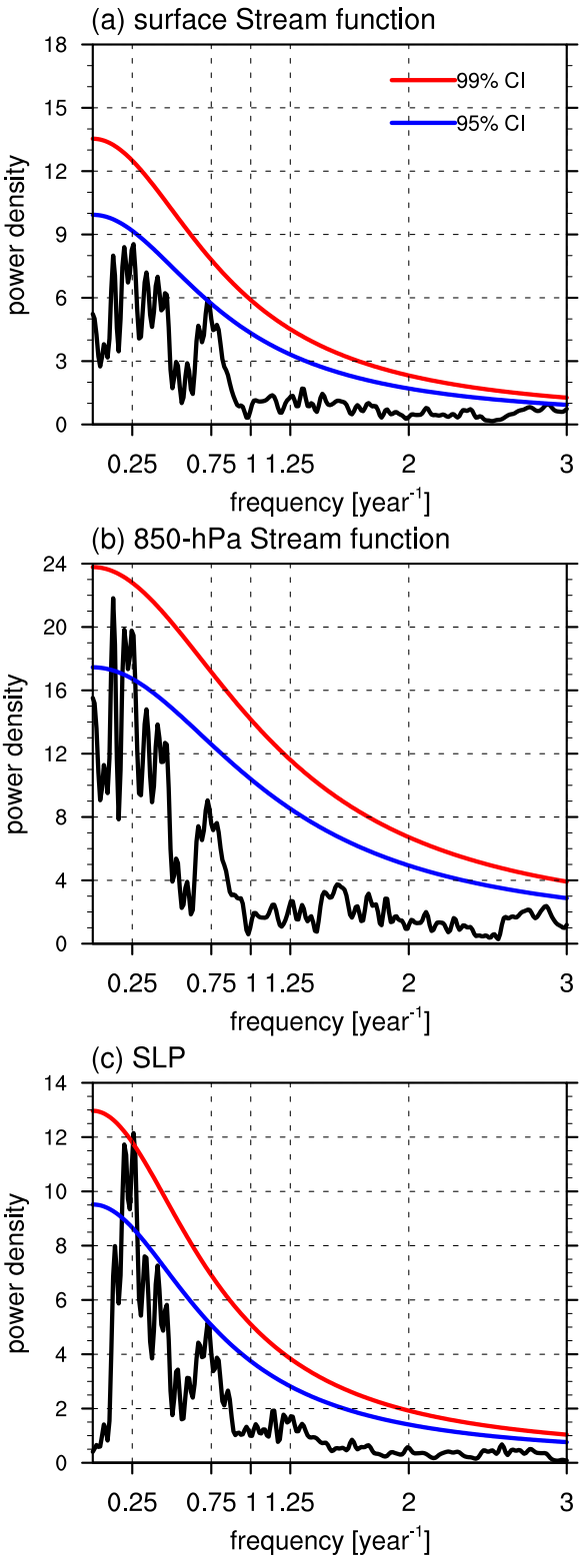


FIG. 2. MTM power spectra for (a) surface streamfunction, (b) 850-hPa streamfunction, and (c) SLP anomalies averaged in the western North Pacific region (5°–20°N, 120°–160°E) during 1980–2001. Black lines indicate the power density and the two colored lines indicate the CI (red = 99% and blue = 95%) based on a red noise null hypothesis.

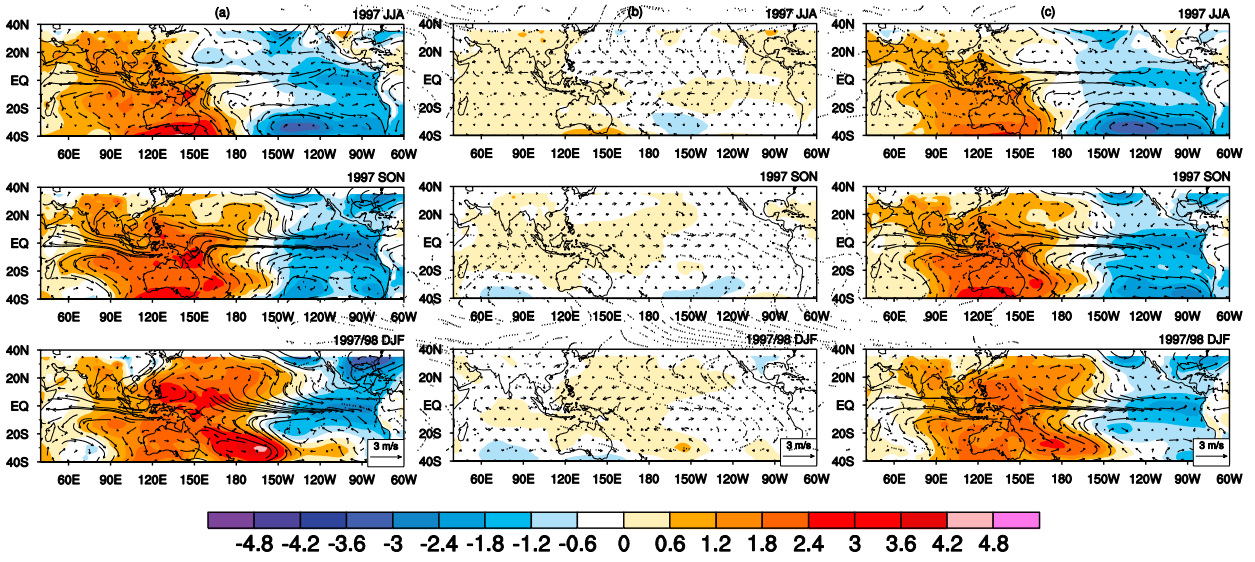


FIG. 3. (a) Seasonal evolution of SLP (shading, hPa) and 850-hPa wind (vectors, $m\,s^{-1}$, reference vector shown in the bottom three panels = $3\,m\,s^{-1}$) anomaly fields from boreal summer to winter in 1997: (top) JJA 1997, (middle) SON 1997, and (bottom) DJF 1997/98. The anomaly fields were derived by subtracting a climatological annual cycle and then applying a 12-month low-pass filter. (b),(c) As in (a), but for 13–19-month and 19–84-month bandpass-filtered anomalies, respectively. The Butterworth filter (Russell 2006) was applied in the above calculations.

Results in Fig. 1 indicate that none of these regions exhibits significant spectrum peaks at the C-mode frequencies in the SLP field. More specifically, no significant peaks are found near the $1.2\,yr^{-1}$ frequency. The same is true for the $0.8\,yr^{-1}$ frequency except in the WNP where a weak spectral peak at $0.8\,yr^{-1}$ is seen, but this peak hardly passes a 0.05 confidence level. Similar results are found in the 850-hPa and surface streamfunction fields (figures not shown).

The power spectrum analysis result is further shown in the WNP region (5°–20°N, 120°–160°E) for different variables (Fig. 2). Both SLP and 850-hPa streamfunction fields exhibit a dominant peak at the interannual (around 2–7 yr) period that is statistically significant at 0.05 confidence level. The spectrum peak around $0.8\,yr^{-1}$ frequency is secondary and not significant at a 0.05 confidence level. The surface streamfunction anomaly, which was used in S15, however, does not pass the 95% significance level at both the ENSO and the $0.8\,yr^{-1}$ frequencies. No clear peaks stand out at the $1.2\,yr^{-1}$ frequency in all these fields.

To examine whether the power spectrum analysis result above is sensitive to analysis period, we conducted an additional calculation with a longer period (1958–2001) of ERA-40 reanalysis data. The results are essentially same. No statistically significant peaks are found at the near-annual frequencies anticipated by the C-mode theory.

In summary, the power spectrum analysis does not detect the near-annual frequencies in the Indo-Pacific low-level circulation fields. The $1.2\,yr^{-1}$ peak is absent across the Indo-Pacific, while a weak $0.8\,yr^{-1}$ peak is seen only in the WNP and such a peak is statistically insignificant. Thus, marked discrepancy exists in the dominant periodicity between the C-mode and the observed circulation anomalies over the tropical Indo-Pacific.

## 3. How much observed WNPAC variability can the C-mode explain?

One might ponder whether the lack of C-mode frequencies is due to the dominance of the low-frequency ENSO variability. Thus, we further examine how much of the observed SLP and low-level circulation variability in the WNP can be attributed to the near-annual mode. Since the 10-month mode was not detected (Fig. 1), we focus on the 15-month mode.

Figure 3 shows the evolution patterns of the observed low-pass-filtered SLP and 850-hPa wind anomalies from boreal summer to winter in 1997 (left panel) and those associated with the 15-month mode (middle panel, derived from a 13–19-month bandpass filter) and the interannual component (right panel, derived from a 19–84-month bandpass filter). Note that the near-annual component only explains 13% of the observed SLP anomaly amplitude averaged in the WNP box (5°–20°N, 120°–160°E), whereas the interannual component explains 77% of the total amplitude. A similar amplitude ratio (13%–15%) is found for other tropical regions and for other variables (e.g., 850-hPa wind anomaly field).

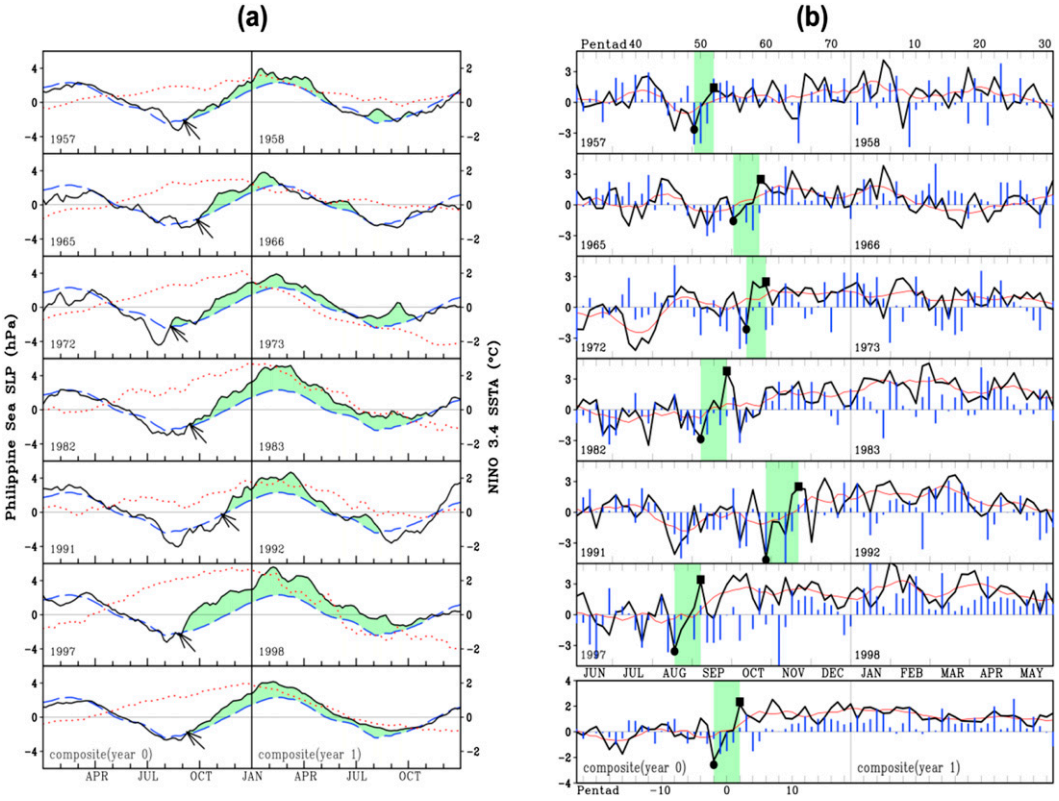


FIG. 4. (a) The 7-pentad running mean (excluding the annual mean; solid black) and the climatological annual cycle (long dashed blue) SLP averaged over the western North Pacific region (10°–20°N, 120°–150°E) for (from top to bottom) the six major El Niño episodes and their composite. The red dotted curves are the corresponding 3-month running mean Niño-3.4 SST anomalies. The arrows point to the time that the anomalous WNPAC occurs. The green shading highlights the period during which the WNPAC persists. (b) Pentad mean anomaly (excluding the annual cycle; thick black) and the corresponding 7-pentad running mean anomaly (thin red) of the SLP averaged over 10°–20°N, 120°–150°E for (from top to bottom) the six major El Niño episodes and their composite. The green intervals mark the transition phase of the establishment period of the anomalous WNPAC. The filled circle and square represent, respectively, the low and high pressure phases of the ISO associated with the formation of the WNPAC. The blue vertical bars at each pentad denote the meridional wind anomalies (m $s^{-1}$) averaged over 15°–30°N, 110°–130°E. The tick marks at the top of the top six and the bottom panels denote Julian pentad. The figure is adapted from Figs. 1 and 3 of Wang and Zhang (2002).

Another way is to compare the variance ratio of monthly time series of the 15-month mode and the observed SLP anomaly averaged in the WNP box from 1980 to 2001. Our calculation shows that the variance ratio is 16%. The weak amplitude of the C-mode could be inferred from the comparison of amplitude of a regressed SLP anomaly [see Fig. 3h of Stuecker et al. (2016), hereafter S16], which is estimated at an average value of 0.6–0.7 hPa over the WNP box, and actual amplitude of the WNP SLP anomaly (around 2–3 hPa) during El Niños (see Figs. 4 and 5).

## 4. Discrepancies in the onset timing of WNPAC between the C-mode and observations

Previous works have addressed specifically how and when the WNPAC was established during El Niño events. By analyzing observational data, Wang and Zhang (2002) showed that the WNPAC formed in northern fall, about one season prior to the peak El Niño (Fig. 4a). They further showed that the WNPAC establishment is abrupt, coupled with a swing from a wet to a dry phase of an intraseasonal oscillation (ISO) (Fig. 4b). The rapid establishment process was found concurrent with early invasion of East Asian cold air break into the Philippine Sea during El Niño developing years. With numerical model experiments that included air–sea interaction in the Indian Ocean and western Pacific, Lau and Nath (2006) demonstrated that the model captured the abrupt establishment of a strong WNPAC anomaly in the autumn of El Niño developing year, which is consistent with the observational analysis of Wang and Zhang (2002). Lau and Nath (2006) further showed that the onset of the WNPAC was accompanied with cold surge and ISO episodes.

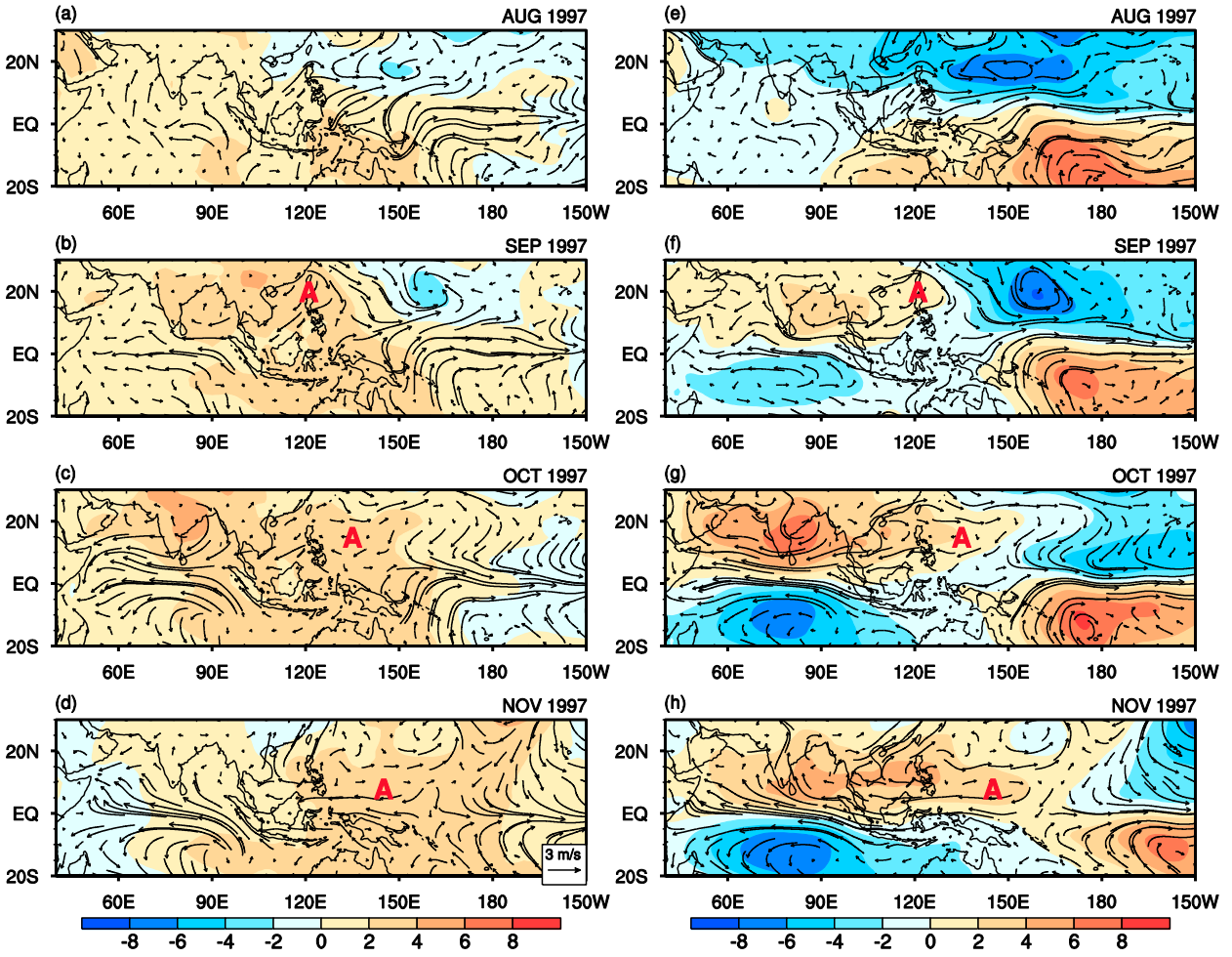


FIG. 5. (a)–(d) August–November 1997 evolution patterns of observed SLP (shading, hPa) and 1000-hPa wind (vectors, $m\,s^{-1}$) anomalies and (e)–(h) observed 850-hPa streamfunction (shaded, $10^6\,m^2\,s^{-1}$) and wind (vectors, $m\,s^{-1}$) anomalies. The WNPAC is marked by a red A in each panel. The reference wind vector ($=3\,m\,s^{-1}$) is shown in (d).

Figure 5 shows the monthly evolutions of horizontal patterns of observed SLP and 1000-hPa wind anomalies (Fig. 5, left) and 850-hPa wind and streamfunction anomalies (Fig. 5, right) from August to November 1997. It is clear that an anomalous low-level anticyclone (AC) emerged over the Philippines in September 1997. By October the anomalous AC covered almost the entire WNP (Figs. 5c,g). In contradiction to the observed onset timing of the anomalous AC in September, the C-mode predicted occurrence of the WNPAC in December 1997 (Fig. 6a; also see Fig. 11 of S15). Note that the C-mode time series had a zero-cross point in November (Figs. 6a,b), meaning that a cyclonic anomaly occurred in WNP prior to November and an AC anomaly occurred in December. Given a relatively short life span of the C-mode, a 3-month phase difference is remarkably large. Thus, clear discrepancies exist between the observation and the C-mode in the onset timing of the WNPAC. The marked difference in the onset timing implies that key physical processes that triggered the WNPAC onset are missing in the C-mode theory.

## 5. Roles of the atmosphere–ocean interaction

S15 claimed that local atmosphere–ocean interaction (AOI) was of secondary importance in the development and maintenance of the WNPAC. Here we show that such a claim contradicts the authors' own numerical modeling result.

We first examine the observed patterns of composite surface streamfunction anomaly and sea surface temperature anomaly (SSTA) fields during El Niño mature winter [December–February (DJF)] (Fig. 7a). Note that the circulation pattern west of 120°E was approximately symmetric about the equator—the opposite signs between the two hemispheres represent the same anticyclonic anomalies. This anticyclonic pair was a direct

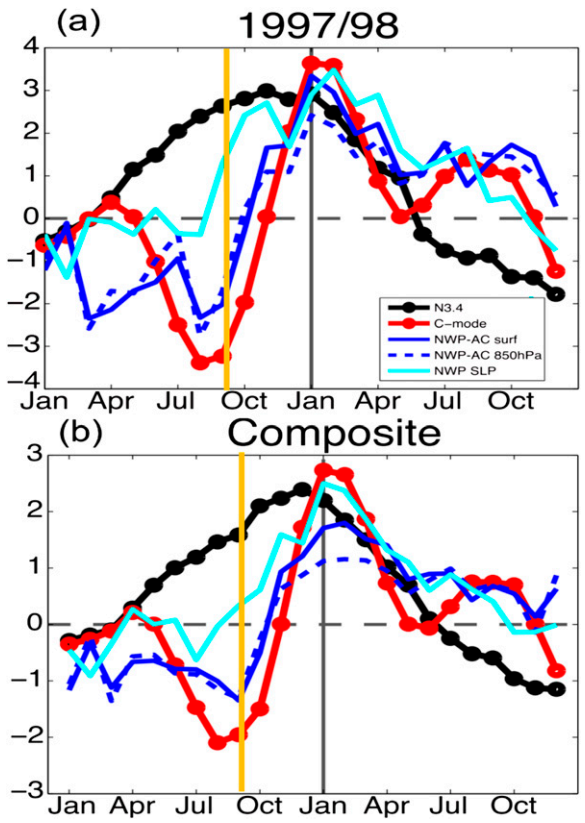


FIG. 6. Time evolution of normalized Niño-3.4 index (black line), theoretical C-mode (red line), WNP (5°–20°N, 120°–160°E) surface streamfunction anomaly (solid blue line), WNP 850-hPa streamfunction anomaly (dashed blue line), and WNP SLP anomaly (cyan line) for (a) 1997/98 and (b) five El Niño composite (adopted from Fig. 1 of S16). The vertical yellow line denotes the actual onset month of the WNPAC.

Rossby wave response to a negative heating anomaly over the Maritime Continent, and had set up during the El Niño developing summer. The streamfunction anomalies between 120° and 160°E, however, were highly asymmetric about the equator. The positive center north of the equator represents an AC anomaly in the WNP and is what we refer to as the WNPAC here. Note that the WNPAC was located slightly to the west of a local cold SSTA. Such an SSTA–AC spatial phase relationship was a result of local air–sea interaction. On one hand, a Rossby wave response to a negative heating anomaly associated with the cold SSTA enhances the WNPAC; on the other hand, the enhanced WNPAC wind anomalies cool the ocean to its east by enhancing evaporative cooling and cold advection in the presence of northern winter–spring mean flows. Wang et al. (2003) diagnosed surface heat flux anomalies in the region and pointed out that there was a local positive thermodynamic air–sea feedback (primarily through the convection–wind–evaporation–SST feedback).

Two sets of numerical experiments were carried out in S15. In the first set, the annual cycle SST over Indo-Pacific and the eastern equatorial Pacific SSTA associated with El Niño were specified. In this set of experiments, the ENSO–annual cycle modulation mechanism that causes the C-mode is fully operated because both the ENSO forcing and the annual cycle of SST are imposed but there is no AOI in the warm pool. For simplicity, we call this type of experiments No-AOI experiments. In the second set, the AOI is allowed in the Indo-Pacific warm pool region (west of the date line) in addition to specified ENSO related SSTA forcing in the eastern Pacific. For simplicity, we name this group of experiments AOI experiments.

In contrast to the observed circulation feature, the No-AOI experiment shows no clear signals of an anomalous AC center east of 120°E during El Niño peak phase (DJF) (Fig. 7b herein, adopted from Fig. 7b of S15). Obviously, the ENSO–annual cycle interaction in the No-AOI experiments failed to simulate the observed circulation asymmetry over the WNP longitudes (120°–160°E) during the El Niño peak winter.

In contrast, the AOI experiments produced a pronounced circulation asymmetry relative to the equator in the Maritime Continent–western Pacific sector (Fig. 7c, adopted from Fig. 8b of S15). The positive streamfunction anomaly center over the northern IO in the No-AOI run has shifted eastward, and the eastern edge of the positive streamfunction anomaly extends from 120° to 150°E. Such a spatial pattern is in significantly better agreement with observations (Fig. 7a) than the pattern obtained in the No-AOI run (Fig. 7b). The eastward shift of the anomalous AC center due to the AOI effect as seen in Fig. 7c confirms the previous coupled model results by Lau et al. (2004) and Lau and Nath (2006). In contrast to the No-AOI run, negative SSTAs formed in the WNP due to AOI. The negative SSTAs were located to the east of the WNPAC and were in good agreement with observations. As elucidated earlier, this spatial phase relationship is a manifestation of AOI.

The observed and simulated circulation features in 1997 (Fig. 7, right; Figs. 7e,f are adopted from Fig. 6 of S16) are generally similar to those shown in the left panel of Fig. 7. In the absence of AOI, the anomalous AC center is confined to the west of 120°E. In the presence of AOI, the anomalous AC center shifts eastward, aligning with the local negative SSTA in the WNP. Thus, it is the AOI, rather than ENSO/annual cycle modulation, that is primarily responsible for the formation of the anomalous anticyclonic center over the Philippine Sea.

## 6. Summary and discussion

The results shown in sections 2–5 suggest that several main conclusions made by S15 are not substantiated. First,

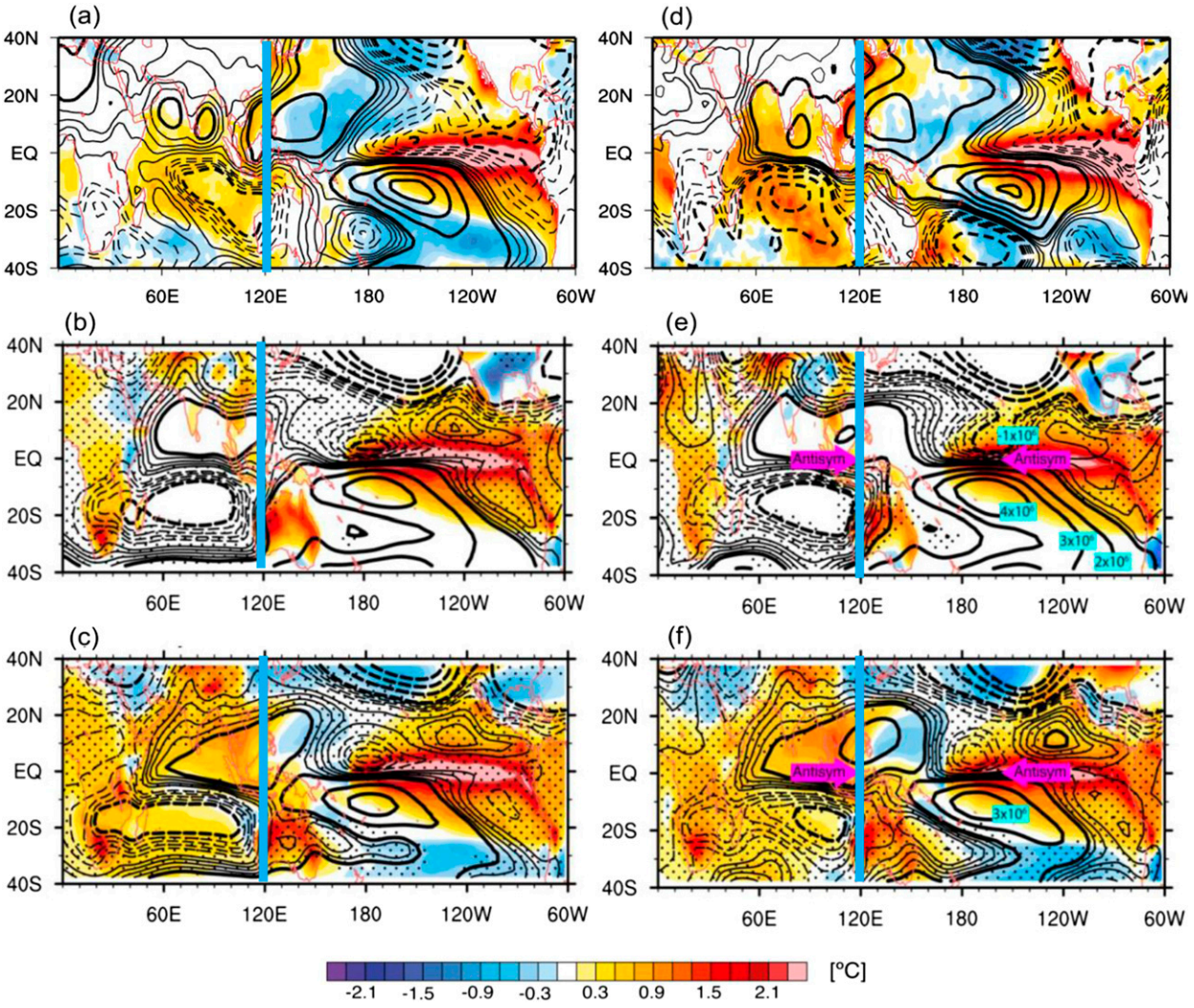


FIG. 7. (a) Observed composite patterns of SST anomalies (shaded, °C) and surface streamfunction anomalies (thin contour interval: $0.2 \times 10^6$ from $-0.8 \times 10^6$ to $0.8 \times 10^6$ m$^2$ s$^{-1}$ and thick contour interval: $10^6$ m$^2$ s$^{-1}$) for El Niño peak phase (DJF) during 1980–2001 (here 1982/83, 1991/92, and 1997/98 cases are used for composite). The SST is from the monthly Hadley Centre Sea Ice and SST dataset (HadISST; Rayner et al. 2003). (b),(c) As in (a), but for the No-AOI and AOI experiments, respectively. (d)–(f) As in (a)–(c), but for 1997/98 DJF season. In all these experiments, the SST anomalies in the tropical eastern Pacific were specified. Areas where the circulation is statistically significant above the 95% confidence level are nonstippled. (b) and (c) Are adapted from Figs. 7b and 8b in S15; (e) and (f) are adapted from Figs. 4b and 4c in S16.

the power spectrum of the circulation anomaly over the WNP is dominated by an interannual (2–7 yr) period. No significant peak is seen in the 1.2 yr$^{-1}$ frequency (hardly passing a 90% confidence level) across the entire tropical Indo-Pacific. The 0.8 yr$^{-1}$ peak is also not seen except over the WNP where the peak hardly passes a 95% confidence level. Second, we show that the circulation anomaly associated with the 0.8 yr$^{-1}$ mode (at a period of 13–19 months) explains only a small portion (13%–15%) of the observed SLP anomaly amplitude over the WNP during 1997 El Niño. For the entire analysis period of 1980–2001, this near-annual mode explains about 16% of the observed SLP variance in the WNP. Third, the C-mode does not describe the observed timing of the WNPAC onset in northern fall. The onset timing described by the C-mode is delayed by about 3 months. Fourthly, we show, based on the previous observational and modeling studies and the authors' own modeling results (Figs. 7b,c,e,f), that local atmosphere–ocean interaction in the WNP does play a role in shifting the anomalous WNPAC center east of Philippines.

To stimulate further studies, we would like to point out that while the C-mode predicts two near-annual frequencies, S15 did not explain why in their observational analysis the 1.2 yr$^{-1}$ peak was hardly seen (Fig. 3a in S15). In their schematic diagram Fig. 12b, S15 did not explain

what causes the westward shift of a northern branch AC cell in the Pacific compared to an anomalous cyclonic cell south of the equator. Yet, understanding such a longitudinal shift is critical if one wants to apply the mathematically derived C-mode theory to a real physical phenomenon such as the formation of the WNPAC.

*Acknowledgments.* This study is supported by China National 973 project 2015CB453200, NSFC Grant 41475084/41375095, ONR Grant N00014-16-1-2260, Jiangsu NSF Key Project BK20150062, and Jiangsu Shuang-Chuang Team 2014SCT001. Bin Wang acknowledges support from the GRL grant of the Korean Ministry of Education, Science and Technology (MEST, 2011-0021927).

## REFERENCES

Chang, C. P., and T. Li, 2000: A theory of the tropical tropospheric biennial oscillation. *J. Atmos. Sci.*, **57**, 2209–2224, doi:10.1175/1520-0469(2000)057<2209:ATFTTT>2.0.CO;2.

Chowdary, J. S., S.-P. Xie, J.-Y. Lee, Y. Kosaka, and B. Wang, 2010: Predictability of summer northwest Pacific climate in 11 coupled model hindcasts: Local and remote forcing. *J. Geophys. Res.*, **115**, D22121, doi:10.1029/2010JD014595.

——, ——, J.-J. Luo, J. Hafner, S. Behera, Y. Masumoto, and T. Yamagata, 2011: Predictability of northwest Pacific climate during summer and the role of the tropical Indian Ocean. *Climate Dyn.*, **36**, 607–621, doi:10.1007/s00382-009-0686-5.

——, C. Gnanaseelan, and S. Chakravorty, 2013: Impact of northwest Pacific anticyclone on the Indian summer monsoon region. *Theor. Appl. Climatol.*, **113**, 329–336, doi:10.1007/s00704-012-0785-9.

Ghil, M., and Coauthors, 2002: Advanced spectral methods for climatic time series. *Rev. Geophys.*, **40**, 1003, doi:10.1029/2000RG000092.

Kosaka, Y., S.-P. Xie, N.-C. Lau, and G. A. Vecchi, 2013: Origin of seasonal predictability for summer climate over the northwestern Pacific. *Proc. Natl. Acad. Sci. USA*, **110**, 7574–7579, doi:10.1073/pnas.1215582110.

Lau, N.-C., and M. J. Nath, 2006: ENSO modulation of the interannual and intraseasonal variability of the East Asian monsoon—A model study. *J. Climate*, **19**, 4508–4530, doi:10.1175/JCLI3878.1.

——, and B. Wang, 2006: Interactions between the Asian monsoon and the El Niño/Southern Oscillation. *The Asian Monsoon*, B. Wang, Ed., Springer/Praxis, 479–512.

——, M. J. Nath, and H. Wang, 2004: Simulations by a GFDL GCM of ENSO-related variability of the coupled atmosphere–ocean system in the East Asian monsoon region. *East Asian Monsoon*, C.-P. Chang, Ed., World Scientific, 271–300.

Li, T., Y. Zhang, C.-P. Chang, and B. Wang, 2001: On the relationship between Indian Ocean SST and Asian summer monsoon. *Geophys. Res. Lett.*, **28**, 2843–2846, doi:10.1029/2000GL011847.

——, P. Liu, X. Fu, B. Wang, and G. A. Meehl, 2006: Spatiotemporal structures and mechanisms of the tropospheric biennial oscillation in the Indo-Pacific warm ocean regions. *J. Climate*, **19**, 3070–3087, doi:10.1175/JCLI3736.1.

Meehl, G. A., 1987: The annual cycle and interannual variability in the tropical Pacific and Indian Ocean region. *Mon. Wea. Rev.*, **115**, 27–50, doi:10.1175/1520-0493(1987)115<0027:TACAIV>2.0.CO;2.

——, 1994: Coupled land–ocean–atmosphere processes and South Asian monsoon variability. *Science*, **266**, 263–267, doi:10.1126/science.266.5183.263.

——, 1997: The South Asian monsoon and the tropospheric biennial oscillation. *J. Climate*, **10**, 1921–1943, doi:10.1175/1520-0442(1997)010<1921:TSAMAT>2.0.CO;2.

Nicholls, N., 1978: Air–sea interaction and the quasi-biennial oscillation. *Mon. Wea. Rev.*, **106**, 1505–1508, doi:10.1175/1520-0493(1978)106<1505:ASIATQ>2.0.CO;2.

Rayner, N. A., D. E. Parker, E. B. Horton, C. K. Folland, L. V. Alexander, D. P. Rowell, E. C. Kent, and A. Kaplan, 2003: Global analyses of sea surface temperature, sea ice, and night marine air temperature since the late nineteenth century. *J. Geophys. Res.*, **108**, 4407, doi:10.1029/2002JD002670.

Russell, D. R., 2006: Development of a time-domain, variable-period surface-wave magnitude measurement procedure for application at regional and teleseismic distances, Part I: Theory. *Bull. Seismol. Soc. Amer.*, **96**, 665–677, doi:10.1785/0120050055.

Stuecker, M. F., A. Timmermann, F.-F. Jin, S. McGregor, and H.-L. Ren, 2013: A combination mode of the annual cycle and the El Niño/Southern Oscillation. *Nat. Geosci.*, **6**, 540–544, doi:10.1038/ngeo1826.

——, F.-F. Jin, A. Timmermann, and S. McGregor, 2015: Combination mode dynamics of the anomalous northwest Pacific anticyclone. *J. Climate*, **28**, 1093–1111, doi:10.1175/JCLI-D-14-00225.1.

——, ——, ——, and ——, 2016: Reply to "Comments on 'Combination mode dynamics of the anomalous northwest Pacific anticyclone.'" *J. Climate*, **29**, 4695–4706, doi:10.1175/JCLI-D-15-0558.1.

Uppala, S. M., and Coauthors, 2005: The ERA-40 Re-Analysis. *Quart. J. Roy. Meteor. Soc.*, **131**, 2961–3012, doi:10.1256/qj.04.176.

Wang, B., and Q. Zhang, 2002: Pacific–East Asian teleconnection. Part II: How the Philippine Sea anomalous anticyclone is established during the El Niño development. *J. Climate*, **15**, 3252–3265, doi:10.1175/1520-0442(2002)015<3252:PEATPI>2.0.CO;2.

——, R. Wu, and X. Fu, 2000: Pacific–East Asian teleconnection: How does ENSO affect East Asian climate? *J. Climate*, **13**, 1517–1536, doi:10.1175/1520-0442(2000)013<1517:PEATHD>2.0.CO;2.

——, ——, and T. Li, 2003: Atmosphere–warm ocean interaction and its impact on Asian–Australian monsoon variation. *J. Climate*, **16**, 1195–1211, doi:10.1175/1520-0442(2003)16<1195:AOIAII>2.0.CO;2.

——, B. Xiang, and J.-Y. Lee, 2013: Subtropical high predictability establishes a promising way for monsoon and tropical storm predictions. *Proc. Natl. Acad. Sci. USA*, **110**, 2718–2722, doi:10.1073/pnas.1214626110.

Webster, P. J., V. O. Magaña, T. N. Palmer, J. Shukla, R. A. Tomas, M. Yanai, and T. Yasunari, 1998: Monsoons: Processes, predictability, and the prospects for prediction. *J. Geophys. Res.*, **103**, 14 451–14 510, doi:10.1029/97JC02719.

Wu, B., T. Zhou, and T. Li, 2009: Seasonally evolving dominant interannual variability modes of East Asian climate. *J. Climate*, **22**, 2992–3005, doi:10.1175/2008JCLI2710.1.

——, T. Li, and T. Zhou, 2010a: Asymmetry of atmospheric circulation anomalies over the western North Pacific between El Niño and La Niña. *J. Climate*, **23**, 4807–4822, doi:10.1175/2010JCLI3222.1.

——, ——, and ——, 2010b: Relative contributions of the Indian Ocean and local SST anomalies to the maintenance of the western North Pacific anomalous anticyclone during El Niño decaying summer. *J. Climate*, **23**, 2974–2986, doi:10.1175/2010JCLI3300.1.

Xiang, B., B. Wang, W. Yu, and S. Xu, 2013: How can western North Pacific subtropical high intensify from early to late summer? *Geophys. Res. Lett.*, **40**, 2349–2354, doi:10.1002/grl.50431.

Xie, S.-P., K. Hu, J. Hafner, H. Tokinaga, Y. Du, G. Huang, and T. Sampe, 2009: Indian Ocean capacitor effect on Indo–western Pacific climate during the summer following El Niño. *J. Climate*, **22**, 730–747, doi:10.1175/2008JCLI2544.1.